Clays and Clay Minerals, Vol. 67, No. 2:143–153, 2019

REMOVAL EFFICIENCY OF BASIC BLUE 41 BY THREE ZEOLITES PREPARED FROM NATURAL JORDANIAN KAOLIN

Mousa Gougazeh[1,2]*, Fethi Kooli[3], and J.-Ch. Buhl[4]

[1]Geology Department, Taibah University, P.O. Box: 30002, Madinah 41447, Saudi Arabia
[2]Natural Resources and Chemical Engineering, Tafila Technical University, P.O. Box 179, Tafila 66110, Jordan
[3]Community College, Taibah University- Al-Mahd Branch, Mahd Al-Dahb 44112, Saudi Arabia
[4]Institute of Mineralogy, Leibniz University Hannover, Callinstr. 3, D-30167 Hannover, Germany

Abstract—The conventional method of zeolite synthesis involves an expensive hydrothermal step whereby a mixture of a metakaolinite, sodium hydroxide, and water is preactivated by thermal treatment between 400°C and 1000°C. The objective of the current study was to determine whether Jordanian kaolinite could be converted to zeolite materials without thermal pre-activation. The alkaline hydrothermal transformation of kaolinite into hydroxysodalite (HS) was achieved, then followed by a reaction with citric acid and solid sodium hydroxide to obtain Zeolite A, or by adding solid Na_2SiO_3 to prepare zeolite X. These materials were tested for their ability to serve as removal agents for Basic Blue 41 (BB-41) dye from artificially contaminated water, at concentrations ranging from 25 to 1000 mg/L. The maximum removal capacities were estimated using the Langmuir model, with a value of 39 mg/g for hydroxysodalite. Zeolite-X achieved the lowest value (19 mg/g). The feasibility of BB-41 removal was deduced from the Freundlich model for the zeolites studied. The reported low-cost method is proposed as an alternative way to reduce the cost of synthesizing zeolite, and the materials were shown to be potential candidates for the removal of BB-41 dye.

Keywords—Basic Blue 41 · Jordanian Kaolin · Removal · Zeolite A · Zeolite X

INTRODUCTION

Synthetic zeolites have become increasingly important due to their wide range of chemical and physical properties; over recent decades they have been used as adsorbents, molecular sieves, membranes, ion exchangers, and catalysts (Rhodes 2010; Zaarour et al. 2014; Li et al. 2017). Zeolite structures consist of three-dimensional frameworks of SiO_4 and AlO_4 tetrahedra. The aluminum ion (Al) is sufficiently small that it can occupy the position in the center of the tetrahedron of four oxygen atoms and the isomorphous replacement of Si^{4+} by Al^{3+} produces a negative charge in the lattice. The net negative charge is balanced by an exchangeable cation [sodium (Na^+), potassium (K^+), or calcium (Ca^{2+})]. These cations are exchangeable with certain other cations in solution (Barer, 1987). Synthesized zeolites are used commercially due to their purity as crystalline products and the uniformity of particle size. The hydrothermal process is expensive, however, and fails to eliminate negative environmental impacts (Abdullahi et al. 2017). The possible use of natural resources and manufacturing wastes as raw materials for the synthesis of zeolite has been studied (Querol et al. 2002; Hiraki et al. 2009; Johnson & Arshad 2014). The use of waste materials helps to reduce production costs, to reduce environmental problems, and turns waste materials into more useful and valuable products (Dubey et al. 2013). A potential candidate is raw kaolinite. Kaolinite, a 1:1 clay mineral, has the general chemical formula ($Al_2Si_2O_5(OH)_4$); it can be mined in a relatively pure form from kaolin deposits (including some large ones in Jordan), making it an inexpensive source of alumina (Al_2O_3) and silica (SiO_2) (Gougazeh & Buhl 2010). Kaolinite has been used as the source of aluminum and silicon for the synthesis of several types of zeolite (Breck 1974; Barer 1982; Costa et al. 1988; Rees & Chandrasekhar 1993; Zhao et al. 2004; Heller-Kallai & Lapides 2007; Ltaief et al. 2015). Hydroxysodalite rather than other zeolites appears to be the primary product obtained after alkaline hydrothermal conversion of kaolinite, with or without intermediate phases (Madani et al. 1990; Buhl et al. 1997). During the synthesis of zeolites, the base material, kaolinite, must be heated at between 550 and 900°C before it is reacted with an alkali solution. In a more recent study, however (Gougazeh & Buhl 2014), the raw kaolinite was shown to convert to a zeolite material (hydroxysodalite, HS) without the thermal preactivation step. This method is considered to be an energy-saving, less expensive process, that does not generate solid or liquid residues that harm ecological systems.

* E-mail address of corresponding author: dr_eng_mhag@yahoo.com
DOI: 10.1007/s42860-019-00016-1

Synthetic dyes or pigments are used widely in textile industries to color-certain products, creating environmentally hazardous waste. The discharge of dyes from these industries into natural streams and rivers poses severe problems, as dyes are toxic to aquatic life and damaging to the aesthetic nature of the environment (Baughman & Perenich 1988; Chung & Cerniglia 1992; de Sousa et al. 2012; Song et al. 2009). Many methods have been used in dye removal, such as sedimentation, chemical treatment, oxidation, biological treatment, electrochemical methodology, and adsorption (Gupta & Suhas 2009). The adsorption technique using many types of adsorbents is still the most favored method for the removal of contaminants from wastewaters due to its efficiency, potential for high removal capacity, low operational cost, and insensitivity to toxic substances (Nandi et al. 2009; Li et al. 2011; Patel, 2012; Kyzas & Kostoglou, 2014; Yagub et al. 2014). Activated carbon is the most popular adsorbent and has been used with great success. However, use of this method is often limited due to high cost, making the method less popular (Huling et al. 2007; Robinson et al. 2001). Natural zeolites have been observed to be highly effective in reducing dye concentrations, since they have large cation exchange capacities, large surface areas, and large contents of residual carbon (Dubey et al. 2013; Karadag et al. 2007; Ng et al. 2013).

Synthetic zeolites have exchangeable cations which are relatively innocuous (Na^+, Ca^{2+}, and K^+) and tuneable pore sizes that make them particularly suitable for removing undesirable materials from industrial or agricultural effluent (Wang & Peng 2010; Hernández-Montoya et al. 2013; Yuna 2016). From these synthetic materials, zeolite A (ZA) and zeolite X (ZX) were selected for study. Their synthesis, however, is achieved generally from high-cost chemicals, thus limiting their commercial application (Schwanke et al. 2017). The purpose of the present study was to test the hypothesis that zeolites (hydroxysodalite, zeolite A, and zeolite X) could be synthesized using raw kaolinite without prior thermal treatment, and to determine the utility of the synthesized materials by measuring how effective they are at removing BB-41 from artificially contaminated water.

EXPERIMENTAL

Materials

Natural kaolinite was collected from the Jabal Al-Harad kaolin deposit (Batn El-Ghoul area). It is located in southern Jordan, 280 km south of Amman, ~70 km southeast of Ma'an city, and 4 km to the east of the Ma'an–Mudawwara road at latitude 29°37′52″N and longitude 35°20′57″E (Fig. 1; Gougazeh & Buhl 2010). According to Rietveld refinement of X-ray diffraction (XRD) data, the material used in this study for synthesis reactions is ~80 wt.% kaolinite and ~16 wt.% quartz and has a chemical composition of 53.86 wt.% SiO_2, 0.74 wt.% TiO_2, 32.45 wt.% Al_2O_3, 0.65 wt.% Fe_2O_3, 0.08 wt.% MgO, 0.13 wt.% CaO, 0.06 wt.% Na_2O, 0.54 wt.% K_2O and 11.21% LOI (Gougazeh & Buhl 2010).

Sodium hydroxide (NaOH, 99%) as pellets was purchased from Merck Chemical Company (Darmstadt, Germany), citric acid and sodium silicate solution ($Na_2Si_2O_5$) were provided by Fluka Chemie (Buchs, Switzerland), and analytical-grade Basic Blue 41 (BB-41) was purchased from Sigma–Aldrich (Munich, Germany) and used without further purification. BB-41 has the molecular formula $C_{20}H_{26}N_4O_6S_2$ (molecular weight = 482.57 g/mol) with a color index number 11105. The chemical structure of BB-41 is shown in Fig. 2 (Tajul Islam et al. 2015). Distilled water was used in the standard purification methods.

Preparation of Zeolites

The zeolite A was prepared following the method described by Gougazeh & Buhl (2014). 1.0 g of raw kaolinite (RK) was treated in 8 M NaOH at 120°C for 20 h. The product was washed three times using distilled water and dried overnight at 80°C. Then, 1 g of the product, hydroxysodalite, was mixed with diluted citric acid (20 mL 1 M) and heated to ~70°C for 2–4 h. To this solution, solid NaOH powder (3.2 g) was added with vigorous stirring at room temperature for homogenization. The resulting zeolite precursor gel was placed in an autoclave (50 mL) and kept at ~100 °C for 3 h. After hydrothermal treatment, the product was filtered and washed three times with distilled water to remove excess alkali, then oven-dried at 80 °C for 4 h.

The process to prepare zeolite X consisted, firstly, of the alkaline hydrothermal transformation of kaolinite into hydroxysodalite, as described above for zeolite A, followed by the same treatment with diluted citric acid (20 mL 1 M) and heating to ~70°C for 2–4 h. To this solution, 3.2 g (8.0 M) of solid NaOH powder and 0.5 g of solid Na_2SiO_3 powder were added with vigorous stirring at room temperature for homogenization; the pH of the aluminosilicate solution was adjusted to ~12 to obtain a gel; it was then placed in an autoclave (50 mL) and kept at ~80°C for 16 h. After hydrothermal treatment, the product was filtered and washed three times with distilled water to remove excess alkali. Next, the samples were oven-dried at 80°C for 4 h.

Batch Mode Adsorption Studies

The adsorption experiments were performed in a batch process (Kooli et al. 2015b). Preliminary experiments demonstrated that equilibrium was established in ~8 h, but the experiments were allowed to run for 18 h. To obtain adsorption isotherms, a fixed amount (0.100 g) of kaolinite or zeolite was mixed with 10 mL of dye solution of different concentrations from 25 to 1000 mg/L. The supernatant was collected by centrifugation for 10 min at 2380×*g* using a Labofuge 200 centrifuge. The equilibrium BB-41 concentrations were determined by using a Cary 100 Conc spectrophotometer from Varian (Sydney, Australia) at 610 nm.

https://doi.org/10.1007/s42860-019-00016-1 Published online by Cambridge University Press

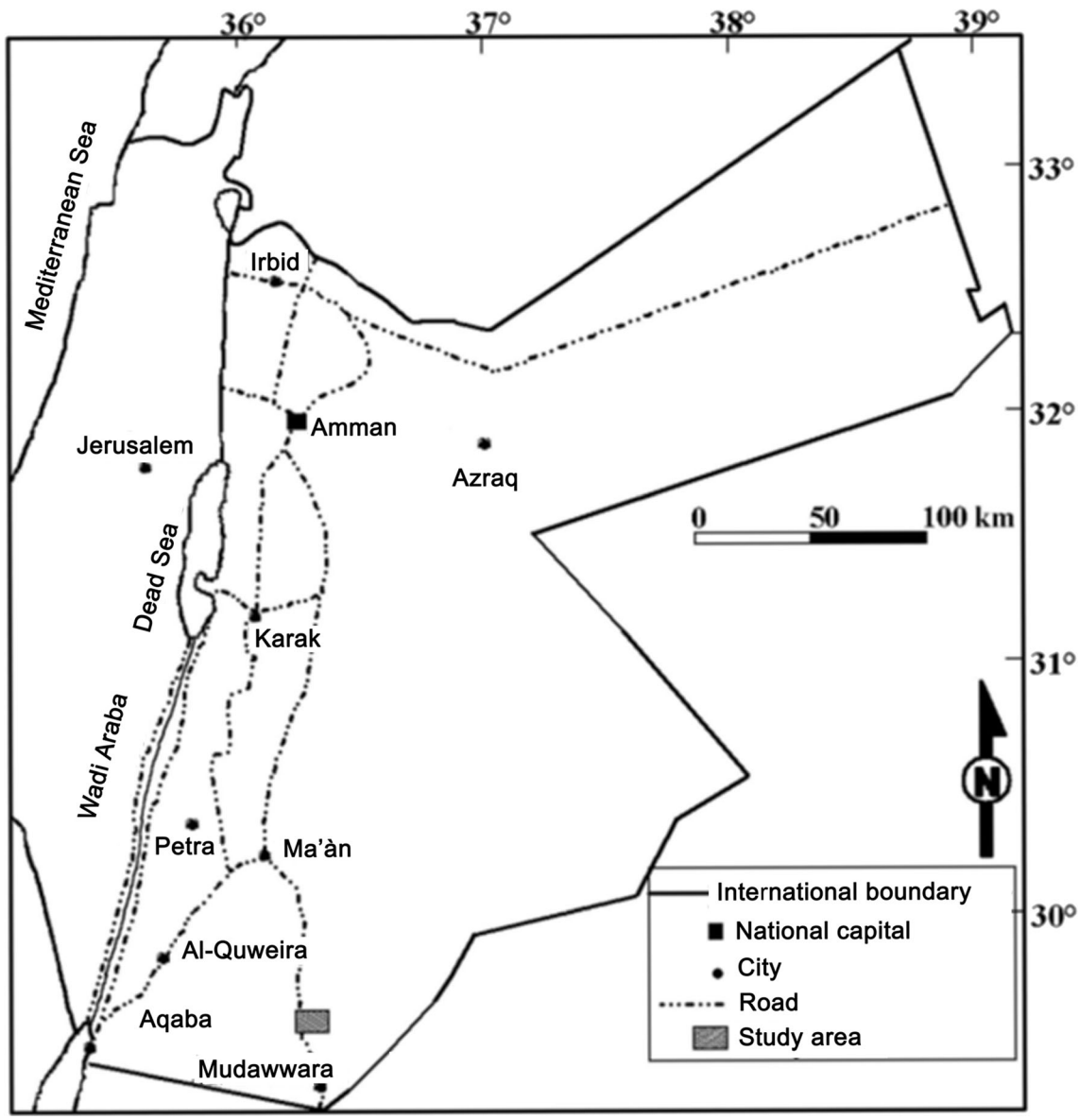

Fig. 1 Location map of the Jabal Al-Harad, Jordan, kaolin deposit

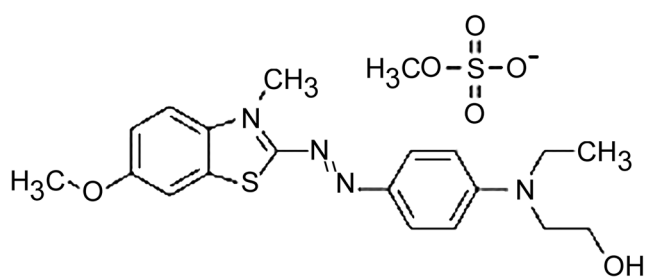

Fig. 2 Chemical structure of the dye Basic Blue 41

https://doi.org/10.1007/s42860-019-00016-1 Published online by Cambridge University Press

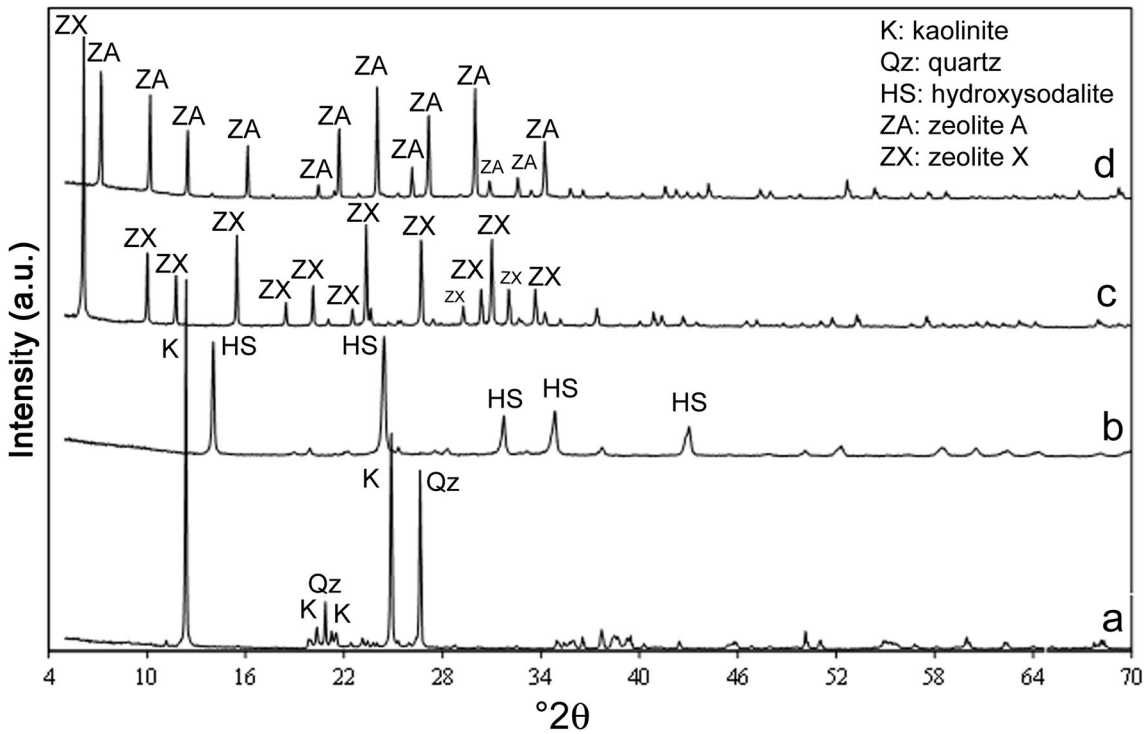

Fig. 3 Powder XRD patterns of the samples, including (**a**) Jordanian kaolinite (JK), (**b**) synthesized hydroxysodalite (HS), (**c**) synthesized zeolite X (ZX), and (**d**) synthesized zeolite A (ZA)

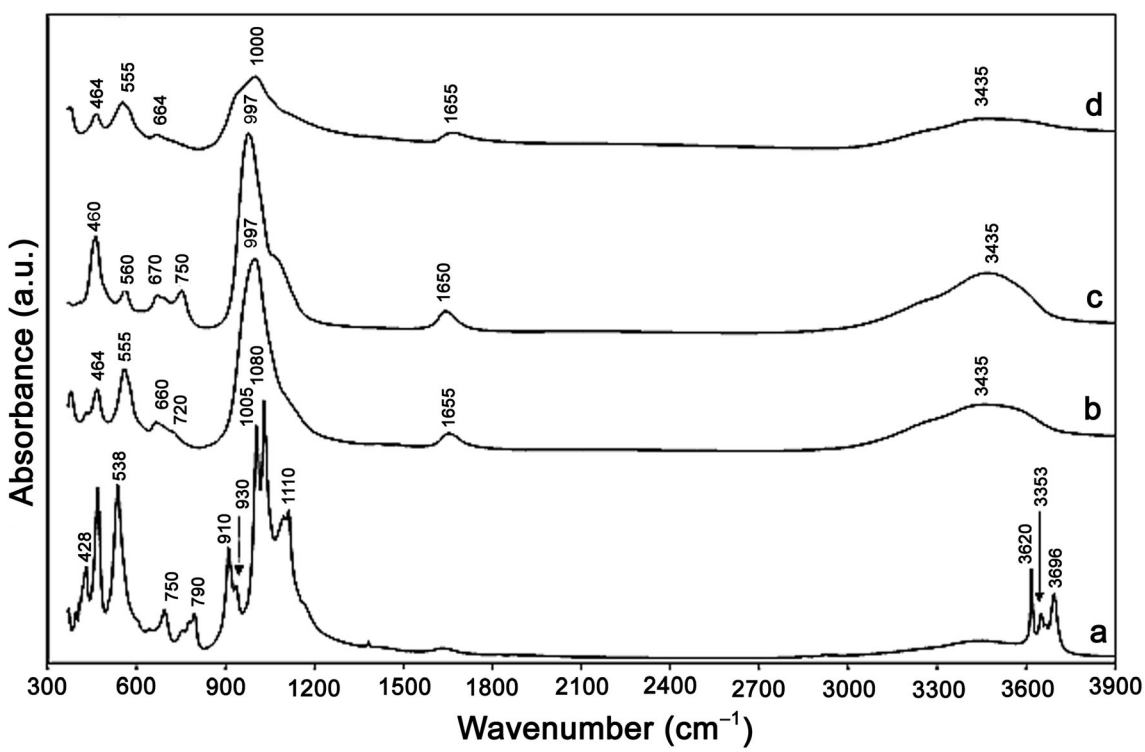

Fig. 4 FTIR spectra of the samples, including (**a**) Jordanian kaolinite, (**b**) synthesized zeolite X (ZX), (**c**) synthesized hydroxysodalite (HS), and (**d**) synthesized zeolite A (ZA)

https://doi.org/10.1007/s42860-019-00016-1 Published online by Cambridge University Press

The removal capacity of dye was calculated as follows:

$$q_e = (C_i - C_e) \times \frac{V}{W} \quad (1)$$

and the removal percentage of dye was calculated as

$$R\% = \frac{(C_i - C_e)}{C_i} \times 100 \quad (2)$$

where q_e (mg/g) is the amount of dye adsorbed, C_i (mg/L) is the initial dye concentration, C_e is the dye concentration at equilibrium, W (g) is the mass of adsorbent added to the BB-41 solution, and V (L) is the volume of the dye solution.

Regeneration Process

The spent materials were regenerated as reported previously (Kooli et al. 2015b). The ZX, ZA, or HS samples were added separately to 10 mL of BB-41 solution (200 ppm) overnight. Each solid was collected by centrifugation and was then dispersed into 10 mL of $Co(NO_3)_2{\cdot}6H_2O$ aqueous solution. The Co^{2+}cations served as a homogeneous catalyst. The oxidant, 10 mg of oxone ($2KHSO_5{\cdot}KHSO_4{\cdot}K_2SO_4$) was added to the mixture to degrade the adsorbed BB-41, via sulfate radical oxidation. The mixture was stirred for 30 min, separated by centrifugation, washed four or five times with deionized water, and then recycled for the next run. The same oxone and $Co(NO_3)_2$ aqueous solution was used throughout the recycle runs.

Characterization

The identification of mineralogical phases comprising the raw kaolinite and the zeolite products was achieved using XRD patterns from a Bruker AXS D4 ENDEVOR diffractometer (Hannover, Germany) with Ni-filtered CuKα radiation at 40 kV and 40 mA. The powder samples were mounted on the sample holder with very little pressure so as to minimize preferred orientation of particles in the sample. The measurements were carried out with a step width of 0.03°2θ and a measuring time of 1 s per step. The powder data were evaluated with the Stoe *WinXPOW* software package. Fourier-transform infrared spectroscopy (FTIR) measurements were performed using a Bruker IFS66v FTIR spectrometer in the 4000–370 cm^{-1} region with samples as KBr pellets. A JEOL JSM-6390A scanning electron microscope (SEM) equipped with a field electron gun (20 kV) was used to study the morphology of the samples. The textural characteristics, such

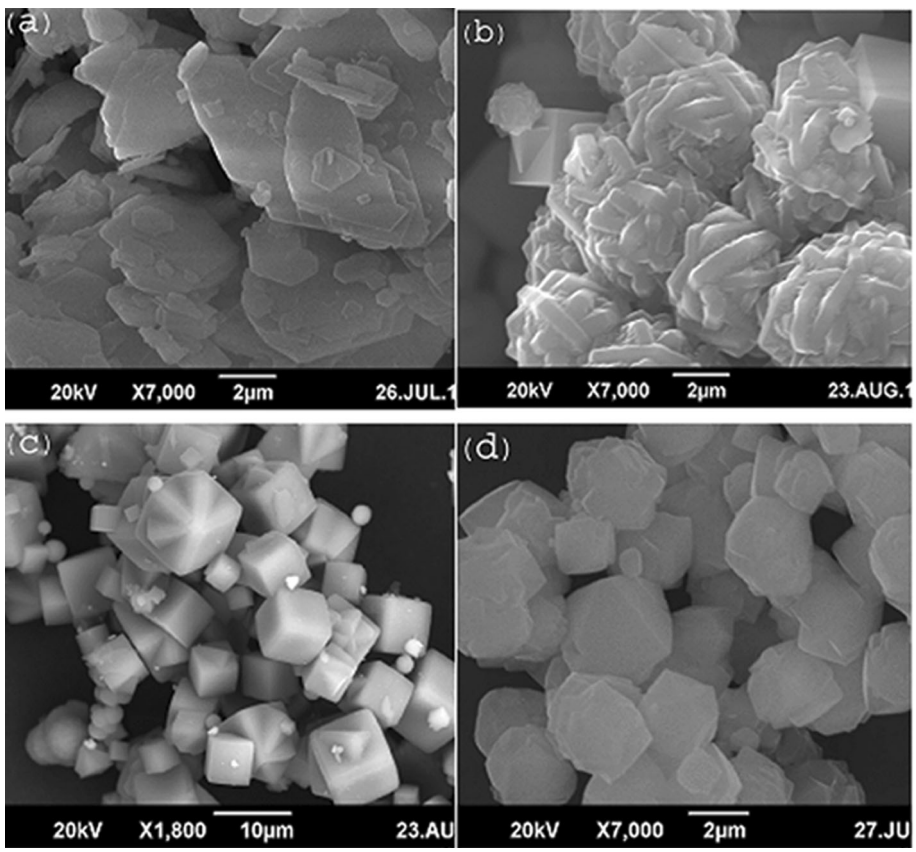

Fig. 5 SEM images of: (**a**) of pseudohexagonal crystals of Jordanian kaolinite; (**b**) spherical (spheroidal) agglomerates of hydroxysodalite grown on the surface of well developed cubes of zeolite A; (**c**) very well defined cubes of zeolite A; and (**d**) well defined crystals of zeolite X

https://doi.org/10.1007/s42860-019-00016-1 Published online by Cambridge University Press

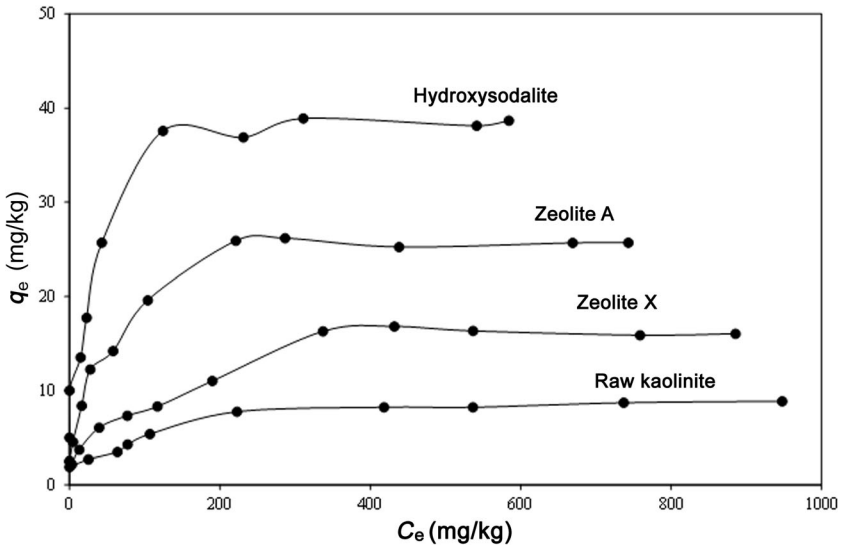

Fig. 6 Basic Blue 41 adsorption isotherms for Jordanian kaolinite, hydroxysodalite, zeolite A, and zeolite X

as specific surface area (S_{BET}), total pore volume (TPV), and average pore diameter of the different samples, were determined from nitrogen adsorption isotherms using a Micromeritics (Norcross, Georgia, USA) ASAP 2040. All samples were degassed at 150°C overnight prior to measurement. The concentrations of the BB-41 dye after treatment with the kaolinite and zeolites were measured by UV-Visible spectroscopy at 610 nm.

RESULTS AND DISCUSSION

X-ray Diffraction

The powder XRD data indicated that the kaolinite exhibited characteristic reflections at 12.35°2θ (001) and 24.64°2θ (002) with additional ones related to quartz (Fig. 3a), and the H-S material showed several common reflections at 14.10 (110), 19.98 (200), 24.54 (211), 31.85 (310), and 34.99°2θ (222) (Fig. 3b), as reported in previous studies (Lee et al. 2003; Gougazeh & Buhl 2014). The products synthesized products (ZA and ZX) exhibited high crystallinity and purity, as no impurities were detected. ZX exhibited several common reflections detected at 2θ values of 6.10° (111), 9.99° (220), 11.74° (311), 15.45° (331), 18.44° (511), 20.10° (440), 23.32° (537), 26.70° (642), 30.47° (660), 31.15° (751), 32.03° (840), and 33.62° (864) (Fig. 3c). ZA exhibited characteristic reflections located at 7.14° (100), 10.10° (110), 12.38° (111), 16.38° (210), 21.58° (300), 23.92° (311), 27.00° (321), 29.82° (410), and 34.08° (332) °2θ (Fig. 3d; Gougazeh & Buhl 2014).

Table 1 Langmuir parameters for the removal of BB-41 by the samples studied

Samples	q_{max}(mg/g)	K_L(L/mg)	R2
RK	6.21	0.0052	0.95
HS	39.37	0.085	0.9975
ZX	17.69	0.0142	0.9842
ZA	26.80	0.0392	0.9968

RK, Raw kaolinite; HS, Hydroxysodalite; ZA, Zeolite A; ZX, Zeolite X

FTIR Spectroscopy

The structural changes that occurred during synthesis were monitored by FTIR spectroscopy (Fig. 4). The IR spectra show the prominent peaks of raw kaolinite (Fig. 3a): 3620–3700 cm^{-1} for -OH stretching, 1000–1120 cm^{-1} for Si–O stretching, 910–940 cm^{-1} for -OH deformation modes, and 400–550 cm^{-1} for Si–O–Si bending vibrations (Farmer 1979; Gougazeh & Buhl 2010). The doublet between 3694 and 3619 cm^{-1} is indicative of a well ordered kaolinite structure (Farmer 1979; Russell 1987; Gougazeh & Buhl 2010; Pentrak et al. 2009, 2012). For the synthesized products (Fig. 4b, c, d), the bands with maxima at 3435 and 1655 cm^{-1} were characteristic of vibrations of functional groups of the OH type and were ascribed to water molecules in the zeolitic materials. Similar behavior was observed in previous studies on the synthesis of crystalline zeolites HS, X, and A (Flanigen et al. 1971; Baren et al. 1999a; Alkan et al. 2005; Garrido-Pedrosa et al. 2006), while obtaining the highly crystalline zeolites HS, X, and A.

The strong signal at ~1000 cm^{-1} characterized the asymmetrical T–O–T valence vibrations (T–Si, Al) of the aluminosilicate zeolite A framework, and the band at ~550 cm^{-1} represented the double ring vibration of the structure (Flanigen et al. 1971). The bands at ~664 cm^{-1} (symmetric stretching mode) and 460 cm^{-1} (T–O bending mode) corresponded to the internal vibrations of the TO_4 tetrahedra (Fig. 3b, c, d). The broader signals at ~550 cm^{-1} and 1000 cm^{-1} of the reaction products characterized silica gel in the mixture with zeolite A, and were another indication of the formation of an amorphous material from the quartz content of the kaolinite (see the XRD paragraph). The additional vibrations in

https://doi.org/10.1007/s42860-019-00016-1 Published online by Cambridge University Press

Table 2 Freundlich parameters for the removal of BB-41 by the samples studied

Samples	1/n	K_F	R2
RK			
HS	0.1859	2.4934	0.8681
ZX	0.3806	0.3686	0.9747
ZA	0.2899	1.4676	0.9467

RK, Raw kaolinite; HS, Hydroxysodalite; ZA, Zeolite A; ZX, Zeolite X

the 720–660 cm^{-1} range were in good agreement with the symmetric stretching modes of hydroxysodalite (729, 701, and 660 cm^{-1}) reported by Flanigen et al. (1971) (Fig. 3c, d). In the same manner, the band near 420 cm^{-1} and the intensive mode at 464 cm^{-1} also indicated the presence of hydroxysodalite in this sample (Fig. 3c); these findings were in good agreement with the reported values of the T–O bending modes of the hydroxysodalite framework structure (Flanigen et al. 1971). The detailed FTIR assignments for hydroxysodalite were summarized by Barnes et al. (1999) and later by Zhao et al. (2004). The broad bands at ~3435 cm^{-1} and 1655 cm^{-1} were attributed to zeolite water (Fig. 3c, d). The synthesized zeolite X showed adsorption bands at 972, 560, and 460 cm^{-1} related to external linkage of the zeolite structure (Somerset et al. 2005). Furthermore, a strong medium band at ~1650 $cm^{-1}$was attributed to the H_2O deformation mode due to incomplete dehydration of the zeolite samples (Fig. 4b). Moreover, the observed single strong band at 3435 cm^{-1} was ascribed to the presence of hydroxyl groups in the faujasite (FAU) supercages (Garrido Pedrosa et al. 2006). Ultimately, the intensities of these adsorption bands were proportionate to the purity of the samples, and were in agreement with the interpretation of the XRD results.

The band at 458 cm^{-1} was close to the band at 456 cm^{-1} (bending vibrations of the TO_4) of FAU zeolite. The bands at 560 and 972 cm^{-1} corresponded to the 6-membered double-ring vibration: to the symmetric stretching and to the asymmetric stretching, respectively. The band at 557 cm^{-1} could represent the beginning of the crystallization of a zeolite with double rings (Gougazeh & Buhl 2014).

Scanning Electron Microscopy

SEM photomicrographs were utilized to determine the microscale structure and morphology of the raw kaolinite and zeolite samples. The progress of the zeolitization reactions was observed through changes in the morphology of the starting material and synthesized products. The SEM photomicrograph of raw kaolinite consisted predominantly of the plate-like morphology and pseudo-hexagonal crystals characteristic of kaolinite (Gougazeh & Buhl 2014; Fig. 5a). The occurrences of hydroxysodalite (HS) crystals growing at the surface of zeolite A and spherical morphologies corresponding to HS associated with cubic crystals of zeolite A can be clearly identified (Gougazeh & Buhl 2014; Fig. 5b). The morphology of the synthesized samples can be observed in the images of zeolite A, with characteristic cubic morphology (Fig. 5c). In contrast, zeolite X exhibited well defined crystals (Fig. 5d).

Adsorption Isotherms

The capacity of raw kaolinite to remove BB-41 was very small and did not exceed 6 mg/g. However, the zeolitic materials exhibited larger removal percentages and capacities (40.9 mg/g for HS, 27.3 mg/g for ZA, and 16.9 mg/g for ZX). For all the samples, the removal percentage of BB-41 decreased as the initial concentration of BB-41 increased. However, the removal capacity of the different zeolites increased as the initial concentrations did (Fig. 6). Similar results were reported using different adsorbents (Adeyemo et al. 2015).

The experimental adsorption data were subjected to Langmuir and Freundlich adsorption isotherm models (Freundlich 1906; Langmuir 1916) to determine the adsorption capacity of the zeolitic materials, and to develop an equation that could be used for design purposes (Ismadji & Bhatia 2000). The Langmuir isotherm represents the equilibrium distribution of dye molecules between the solid and liquid phases. The linearized form allows the calculation of the maximum adsorption capacity (q_{max}) and the Langmuir constant (K_L), and is given by eq. 3:

$$\frac{C_e}{q_e} = \frac{1}{q_{max}.K_L} + \frac{C_e}{q_{max}} \quad (3)$$

where q_e is the amount adsorbed at equilibrium (mg/g), C_e is equilibrium concentration of the adsorbate (mg/L), q_{max} is the maximum amount of dye removed (mg/g), and K_L is related to the energy of adsorption (Langmuir constant, L/mg). These parameters can be calculated from the intercept and slope of the linear plot for the experimental data of C_e/q_e vs. C_e. The isotherms examined fitted well with this model, with R^2 values close to 1 for all of the samples, except for the raw kaolinite. The largest calculated values for q_{max} (Table 1) (the maximum amount or monolayer capacity of BB-41 removed) was for hydroxysodalite (close to 39 mg/g), the smallest value was for

Table 3 Comparison of BB-41 removal by different adsorbents

Adsorbents	RK	HS	ZX	ZA	ZX	ZX
q_{max} (mg/g)	6	39	17	29	39	27
References	This study	This study	This study	This study	Humelnicu et al. (2017)	Selim et al. (2018)

RK, Raw kaolinite; HS, Hydroxysodalite; ZA, Zeolite A; ZX, Zeolite X

https://doi.org/10.1007/s42860-019-00016-1 Published online by Cambridge University Press

Table 4 Textural properties of raw kaolinite and synthesized zeolites

Samples	S_{BET} (m^2/g)	PV (cc/g)	APD (nm)
RK	11	0.027	9.5
HS	26	0.051	7.6
ZX	160	0.145	8.8
ZA	121	0.204	6.7

PV: pore volume; APD: average pore diameter; RK: Raw kaolinite; HS: Hydroxysodalite; ZA: Zeolite A; ZX: Zeolite X

the ZX sample (17.69 mg/g), and for ZA the value was intermediate at 26.9 mg/g. The K_L values indicate the affinity of BB-41 molecules for the zeolite surfaces, and it increased as the q_{max} values increased.

The Freundlich isotherm is an empirical equation which assumes that the adsorption process occurs on heterogeneous surfaces, with a non-uniform distribution of heat of adsorption over the surface (Freundlich 1906). The amount of BB-41 adsorbed (q_e) increased curvilinearly with increasing equilibrium concentration (C_e) but the data did not fit the linear form very well, expressed as

$$\ln q_e = \ln K_F + \frac{1}{n} \ln C_e \quad (4)$$

where K_F (mg/g) and n are the Freundlich constants related to the adsorption capacity, and adsorption intensity of adsorbents, respectively. Values of n in the range $0 < 1/n < 1$ represent favorable adsorption conditions. If a plot of $\ln q_e$ vs. $\ln C_e$ is linear, values of the intercept K_F and the slope 1/n can be obtained. Because the experimental data did not fit the Freundlich equation well for ZA and ZX samples, the R^2 values obtained were far from 1 (Table 2).

Adsorbents such as zeolites consist primarily of silicon and aluminum oxides, the hydroxylated surface of which developed negative charges in aqueous solution (Bertolini et al. 2013). The removal of BB-41 occurred through interaction forces between the negatively charged sites of the adsorbent and the positively charged dye molecules. The removal might have been achieved by cation exchange, when the dye molecule size was appropriate for accessing the pores. The BB-41 molecule is considered a large molecule, however, and could not access the pores of the prepared zeolites (Selim et al. 2018). Indeed, the primary crystalline spherical cavities of a-cages in zeolite A and supercages in zeolite X are 11.4 and 12.6 Å, respectively (Job 2005). Meanwhile, zeolite materials generally display high affinity for cationic dyes with very small molecular size, such as methylene blue (Awala et al. 2016).

A comparison of the maximum removal capacity of BB-41 by various zeolites with similar aluminosilicate structures (Table 3) revealed that the hydroxysodalite prepared has a maximum removal capacity of 39 mg/g, larger than the reported value of 27 mg/g (Selim et al. 2018). This difference could be related to the accessibility of removal sites within the structures of the various zeolite materials or to the specific surface areas of the zeolites used.

The well packed structure of kaolinite makes it difficult for the particles to be broken down, and the layers are not easily separated, so the adsorption properties of kaolinite are likely determined by the edges of the layers (Miranda-Trevinol & Coles 2003).The CEC is confined primarily to the external surface, in contrast to smectites where most of the CEC belongs to interior sites (Miranda-Trevinol & Coles 2003). Kaolinite, consequently, removed less BB-41 than

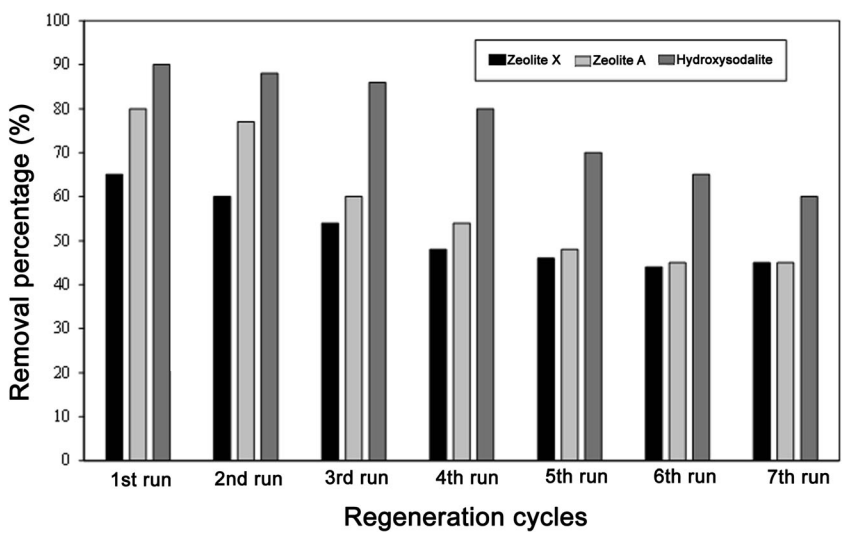

Fig. 7 Regeneration efficiency for (**a**) zeolite A, (**b**) zeolite X, and (**c**) hydroxysodalite after successive regeneration cycles

https://doi.org/10.1007/s42860-019-00016-1 Published online by Cambridge University Press

smectite. In addition, the values obtained were smaller than those reported for some raw clay minerals and acid-activated derivatives (Roulia & Vassiliadis 2005; Kooli et al. 2015a). This difference could be related to the specific surface area or to the accessibility of the adsorbent sites for the BB-41 dye molecules. Indeed, the textural properties of the starting raw kaolinite (RK) and the derived zeolites revealed that the zeolite X and zeolite A exhibited larger surface areas (160 m^2/g and 120 m^2/g, respectively) than hydroxysodalite (26 m^2/g, Table 4). However, small amounts of BB-41 were removed. In this case, the small removal capacities (of BB-41) using both ZX and ZA were probably due to its large size (Selim et al. 2018).

Regeneration Data

The feasibility of applying the adsorbent systems to large-scale operations is determined by either disposal costs of spent adsorbents or regeneration costs. The commonly reported regeneration methods are thermal treatment (Tamon & Okazaki 1997: Wang et al. 2006; Vimonses et al. 2009), chemical and solvent regeneration (Martin & Ng 1978), electrochemical regeneration (Narbaitz & Karimi-Jashni 2008), ultrasonic regeneration (Lim & Okada 2005), and wet air oxidation (Shende & Mahajani 2002). An economical method was used to regenerate the spent zeolites, consisting of treating the spent zeolites with a solution in which Co^{2+} cations served as an homogeneous catalyst and the oxidant oxone was used to degrade the BB-41 removed (Anipsitakis et al. 2006; Kooli et al. 2015a).

The regeneration of the spent zeolites (Fig. 7) revealed that the removal efficiency was preserved, but decreased slightly as the number of cycles increased from 1 to 4. A reduction of 10% was observed compared to the fresh zeolite, for hydroxysodalite. The regeneration efficiencies decreased by 30% after five cycles, and reached a lower value of 60% after seven cycles. Meanwhile, the efficiency of spent ZX and ZA was reduced after three cycles by an average of 25%. The reduction of efficiency might be related to deactivation of removal sites, and indicates that the BB-41 could not be released easily from the spent materials after many cycles, especially for ZX and ZA zeolites (Kooli et al. 2015b).

CONCLUSIONS

Natural Jordanian kaolin is a promising source of silicon and aluminum for the synthesis of zeolites. The formation of zeolites was achieved successfully from a Jordanian kaolin without its pre-activation at higher temperatures. Generally, zeolite A and X products obtained through the synthesis process exhibited well developed crystals with uniform particle-size distribution, as shown by SEM. The transformation of kaolinite into various zeolites led to an improvement in the removal of BB-41, the amounts removed depending on the initial concentrations of the BB-41and the types of zeolite materials obtained. The data fitted well to the Langmuir isotherm, with maximum removal capacities of 17, 29, and 39 meq/g for zeolites ZX, ZA, and hydroxysodalite, respectively. The adsorption capacity was only slightly suppressed at lower equilibrium concentrations for zeolite X and at higher concentration for hydroxysodalite and zeolite A. Zeolites prepared from Jordanian kaolin, especially hydroxysodalite, are promising for the treatment of wastes polluted by dyes. The removal efficiency was preserved after four cycles of regeneration for the zeolites used, and it depended on the type of materials with an average reduction of 10 to 30% after four cycles.

ACKNOWLEDGMENTS

The authors are grateful to the Tafila Technical University (TTU), Jordan for technical support of this research work. Special thanks are due to the Institute of Mineralogy, Leibniz University, Hannover, Germany, for allowing the use of research facilities. Thanks also to Prof. Dr. C. Ruscher, Dr. Lars Robben, and Dipl. Geow. Valeriy Petrov for assistance with the acquisition of FTIR and SEM data.

REFERENCES

Abdullahi, T., Harun, Z., & Othman, M. H. D. (2017). A review on sustainable synthesis of zeolite from kaolinite resources via hydrothermal process. *Advanced Powder Technology, 28*, 1827–1840.

Adeyemo, A. A., Adeoye, I. O., & Bello, O. S. (2015). Adsorption of dyes using different types of clay: A review. *Applied Water Science, 7*, 1–26.

Alkan, M., Hopa, C., Yilmaz, Z., & Guler, H. (2005). The effect of alkali concentration and solid/liquid ratio on the hydrothermal synthesis of zeolite NaA from natural kaolin. *Microporous Mesoporous Materials, 86*, 176–184.

Anipsitakis, G. P., Dionysiou, D. D., & Gonzalez, M. A. (2006). Cobalt-mediated activation of Peroxymonosulfate and sulfate radical attack on phenolic compounds. Implications of chloride ions. *Environmental Science and Technology, 40*, 1000–1007.

Awala, H., Leite, E., Saint-Marcel, L., Clet, G., Retoux, R., Naydenova, I., & Mintova, S. (2016). Properties of methylene blue in the presence of zeolite nanoparticles. *New Journal of Chemistry, 40*, 4277–4284.

Barer, R. M. (1982). *Hydrothermal chemistry of zeolites*. London: Academic Press.

Barer, R. M. (1987). *Zeolites and clay minerals as sorbent and molecular sieves*. New York: Academic Press.

Barnes, M. C., Addai-Mensah, J., & Gerson, A. R. (1999a). The mechanism of the sodalite-to- cancrinite phase transformation in synthetic spent Bayer liquor. *Microporous Mesoporous Materials, 31*, 287–302.

Baughman, G. L., & Perenich, T. A. (1988). Fate of dyes in aquatic systems: I. Solubility and partitioning of some hydrophobic dyes and related compounds. *Environmental Toxicology Chemistry, 7*, 183–199.

Bertolini, T. C. R., Izidoro, J. C., Magdalena, C. P., & Fungaro, D. A. (2013). Adsorption of crystal violet dye from aqueous solution onto zeolites from coal fly and bottom ashes. *Orbital Electron Journal Chemistry, 5*, 179–191.

Breck, D. W. (1974). *Zeolite molecular sieves: Structure, chemistry and use*. New York: John Wiley & Sons Inc.

Buhl, J. C., Hoffmann, W., Buckermann, W. A., & Muller-Warmuth, W. (1997). The crystallization kinetics of sodalites grown by the hydrothermal transformation of kaolinite studied by ^{29}Si MAS NMR. *Solid State Nuclear Magnetic Resonance, 9*, 121–128.

Chung, K. T., & Cerniglia, C. E. (1992). Mutagenicity of azo dyes: Structure-activity relationships. *Mutation Research, 277*, 201–220.

Costa, E., De Lucas, A., Uguina, M. A., & Ruiz, J. C. (1988). Synthesis of 4A zeolite from calcined kaolins for use in detergents. *Industrial and Engineering Chemistry Research, 27*, 1291–1296.

Dubey, A., Goyal, D., & Mishra, A. (2013) Zeolites in wastewater treatment. Pp. 82–104 in: Green materials for sustainable water

remediation and treatment (A. Mishra & J.H. Clark, editors). RSC Green Chemistry Series, The Royal Society of Chemistry, Cambridge, UK.

Farmer, V.C. (1979) Infrared spectroscopy. Pp. 285–337 in: Data handbook for clay minerals and other non-metallic minerals (H. van Olphen & J.J. Fripiat, editors). Pergamon Press, New York, USA.

Flanigen, E., Khatami, M., & Szymanski, H. A. (1971). Infrared structural studies of zeolite frameworks. *Advances in Chemistry, 101*, 201–229.

Freundlich, U. (1906). Dye adsorption in lusungen. *Journal of Physical Chemistry, 57*, 385–470.

Garrido Pedrosa, A. M., Souza, M. J. B., Melo, D. M. A., & Araújo, A. S. (2006). Cobalt and nickel supported on HY zeolite: Synthesis, characterization and catalytic properties. *Materials Research Bulletin, 41*, 1105–1111.

Gougazeh, M., & Buhl, J. C. (2010). Geochemical and mineralogical characterization of the Jabal Al-Harad kaolin deposit, southern Jordan, for its possible utilization. *Clay Minerals, 45*, 281–294.

Gougazeh, M., & Buhl, J. C. (2014). Conversion of natural Jordanian kaolin into zeolite a without thermal pre-activation. *Zeitschrift für Anorganische und Allgemeine Chemie, 640*, 1675–1679.

Gupta, V. K., & Suhas (2009). Application of low-cost adsorbents for dye removal-a review. *Journal of Environmental Management, 90*, 2313–2342.

Heller-Kallai, L., & Lapides, I. (2007). Reactions of kaolinites and metakaolinites with NaOH-comparison of different samples (part 1). *Applied Clay Science, 35*, 99–107.

Hernández-Montoya, V., Pérez-Cruz, M. A., Mendoza-Castillo, D. I., Moreno-Virgen, M. R., & Bonilla-Petriciolet, A. (2013). Competitive adsorption of dyes and heavy metals on zeolitic structures. *Journal of Environmental Management, 116*, 213–221.

Hiraki, A., Nosaka, A., Okinaka, N., & Akiyama, T. (2009). Synthesis of zeolite-X from waste metals. *Journal of the Iron and Steel Institute of Japan International, 49*, 1644–1649.

Huling, S. G., Jones, P. K., & Lee, T. R. (2007). Iron optimization for Fenton-driven chemical oxidation of MTBE-spent granular activated carbon. *Environmental Science and Technology, 41*, 4090–4096.

Humelnicu, I., Baiceanu, A., Ignat, M. E., & Dulman, V. (2017). The removal of basic blue 41 textile dye from aqueous solution by adsorption onto natural zeolitic tuff: Kinetics and thermodynamics. *Process Safety and Environmental Protection, 105*, 274–287.

Ismadji, S., & Bhatia, S. K. (2000). Adsorption of flavor esters on granular activated carbon. *Canadian Journal of Chemical Engineering, 78*, 892–901.

Job R (2005) Zeolites and nanoclusters in zeolite host lattices. Pp. 127-142 in: Nanotechnology and nanoelectronics: materials, devices, measurement techniques (Fahrner, W.R. editor). Springer, Berlin.

Johnson, E. B. G., & Arshad, S. E. (2014). Hydrothermally synthesized zeolites based on kaolinite: A review. *Applied Clay Science, 97-98*, 215–221.

Karadag, D., Akgul, E., Tok, S., Erturk, F., Kaya, M. A., & Turan, M. (2007). Basic and reactive dye removal using natural and modified zeolites. *Journal of Chemical & Engineering Data, 52*, 2436–2441.

Kooli, F., Yan, L., Al-Faze, R., & Al-Sehimi, A. (2015a). Effect of acid activation of Saudi local clay mineral on removal properties of basic blue 41 from an aqueous solution. *Applied Clay Science, 116–117*, 23–30.

Kooli, F., Yan, L., Al-Faze, R., & Al-Sehimi, A. (2015b). Removal enhancement of basic blue 41 by waste brick from an aqueous solution. *Arabian Journal of Chemistry, 8*, 333–342.

Kyzas, G., & Kostoglou, M. (2014). Green adsorbents for wastewaters: *A Critical Review. Materials, 7*, 333–364.

Langmuir, I. (1916). The constitution and fundamental properties of solids and liquids. *Journal of the American Chemical Society, 38*, 2221–2295.

Lee, S. R., Han, Y. S., Park, M., Park, G. S., & Choy, J. H. (2003). Nanocrystalline sodalite from Al_2O_3 pillared clay by solid−solid transformation. *Chemistry of Materials, 15*, 4841–4845.

Li, C., Dong, Y., Wu, D., Peng, L., & Kong, H. (2011). Surfactant modified zeolite as adsorbent for removal of humic acid from water. *Applied Clay Science, 52*, 353–357.

Li, Y., Li, L., & Yu, J. (2017). Applications of zeolites in sustainable chemistry. *Chem, 3*, 928–949.

Lim, J. L., & Okada, M. (2005). Regeneration of granular activated carbon using ultrasound. *Ultrasonics Sonochemistry, 12*, 277–282.

Ltaief, O. O., Siffert, S., Poupin, C., Fourmentin, S., & Benzina, M. (2015). Optimal synthesis of Faujasite-type zeolites with a hierarchical porosity from natural clay. *European Journal of Inorganic Chemistry, 28*, 4658–4665.

Madani, A., Aznar, A., Sanz, J., & Serratosa, J. M. (1990). Silicon-29 and aluminum-27 NMR study of zeolite formation from alkali-leached kaolinites: influence of thermal pre-activation. *Journal of Physical Chemistry, 94*, 760–765.

Martin, R. J., & Ng, W. J. (1978). The repeated exhaustion and chemical regeneration of activated carbon. *Water Research, 21*, 961–965.

Miranda-Trevinol, J. C., & Coles, C. A. (2003). Kaolinite properties, structure and influence of metal retention on pH. *Applied Clay Science, 23*, 133–139.

Nandi, B. K., Goswami, A., & Purkait, M. K. (2009). Removal of cationic dyes from aqueous solutions by kaolin: Kinetic and equilibrium studies. *Applied Clay Science, 42*, 583–590.

Narbaitz, R. M., & Karimi-Jashni, A. (2008). Electrochemical regeneration of granular activated carbons loaded with phenol and natural organic matter. *Environmental Technology, 30*, 27–36.

Ng, E.P., Zou, X., and Mintova, S. (2013) Environmental synthesis concerns of zeolites. Pp. 289–310 in: New and future developments in catalysis: Hybrid materials, composites, and organocatalyts (L.S. Suib, editor). Elsevier, Amsterdam.

Patel, S. (2012). Potential of fruit and vegetable wastes as novel biosorbents: Summarizing the recent studies. *Reviews in Environmental Science and Biotechnology, 4*, 365–380.

Pentrak, M., Madejová, J., & Komadel, P. (2009). Acid and alkali treatments of kaolins. *Clay Minerals, 44*, 511–523.

Pentrak, M., Madejová, J., Andrejkovičová, S., Uhlík, P., & Komadel, P. (2012). Stability of kaolin sand from Vyšný Petrovec deposit (South Slovakia) in acid environment. *Geologica Carpathica, 63*, 503–512.

Querol, X., Moreno, N., Umana, J. C., Alastuey, A., Hernandez, E., Lopez-Soler, A., & Plana, F. (2002). Synthesis of zeolites from coal fly ash: An overview. *International Journal of Coal Geology, 50*, 413–423.

Rees, L., & Chandrasekhar, S. (1993). Hydrothermal reaction of kaolin in presence of fluoride ions at pH less than 10. *Zeolites*, (13), 534–541.

Rhodes, C. J. (2010). Properties and applications of zeolites. *Science Progress, 93*, 223–284.

Robinson, T., McMullan, G., Marchant, R., & Nigam, P. (2001). Remediation of dyes in textile effluent: A critical review on current treatment technologies with a proposed alternative. *Bioresources Technology, 77*, 247–255.

Roulia, M., & Vassiliadis, A. A. (2005). Interactions between C.I. Basic blue 41 and aluminosilicate sorbents. *Journal of Colloid and Interface Science, 291*, 37–44.

Russell, J.D. (1987) Infrared methods. Pp. 133–173 in: A Handbook of Determinative Methods in Clay Mineralogy (M.J. Wilson, editor). Chapman & Hall, London.

Schwanke, A.J., Balzer, R., and Pergher, S. (2017) Microporous and mesoporous materials from natural and inexpensive sources. Pp. 1–22 Chapter 1. in: Handbook of Ecomaterials, (L.M.T. Martínez, O.V. Kharissova, and B.I. Khatisov, editors), Springer, Basel.

Selim, M. M., El-Makkawi, D. M., & Ibrahim, F. A. (2018). Innovative synthesis of black zeolites-based kaolin and their adsorption behavior in the removal of methylene blue from water. *Journal of Materials Science, 53*, 3323–3331.

Shende, R. V., & Mahajani, V. V. (2002). Wet oxidative regeneration of activated carbon loaded with reactive dye. *Waste Management, 22*, 73–83.

Somerset, V. S., Petrik, L. F., White, R. A., Klink, M. J., Key, D., & Iwuoha, E. I. (2005). Alkaline hydrothermal zeolites synthesized from high SiO_2 and Al_2O_3 co-disposal fly ash filtrates. *Fuel, 84*, 2324–2329.

Song, L., Chen, F., Hu, J. C., & Richards, R. (2009). NiO (111) nanosheets as efficient and recyclable adsorbents for dye pollutant removal from wastewater. *Nanotechnology, 20*, 275707–275716.

de Sousa, M. L., de Moraes, P. B., Matos Lopes, P. R., Montagnolli, R. N., de Angelis, D., & Bidoia, E. D. (2012). Contamination by Remazol red brilliant dye and its impact in aquatic photosynthetic microbiota. *Environmental Management and Sustainable Development, 1*, 129–138.

Tajul Islam, M., Aimone, F., Ferri, A., & Rovero, G. (2015). Use of N-methylformanilide as swelling agent for meta-aramid fibers dying: Kinetics and equilibrium adsorption of basic blue 41. *Dyes and Pigments, 113*, 554–561.

Tamon, Z. H., & Okazaki, M. (1997). Influence of surface oxides on ethanol regeneration of spent carbonaceous adsorbents. *Journal of Colloid and Interface Science, 196*, 120–122.

Vimonses, V., Jim, B., Chow, C. K. W., & Saint, C. (2009). Enhancing removal efficiency of anionic dye by combination and calcination of clay materials and calcium hydroxide. *Journal of Hazardous Materials, 171*, 941–947.

Wang, S., & Peng, Y. (2010). Natural zeolites as effective adsorbents in water and wastewater treatment. *Chemical Engineering Journal, 156*, 11–24.

Wang, S., Li, H., Xie, S., Liu, S., & Xu, L. (2006). Physical and chemical regeneration of zeolitic adsorbents for dye removal in wastewater treatment. *Chemosphere, 65*, 82–87.

Yagub, M. T., Kanti Sen, T., Afroze, S., & Ang, H. M. (2014). Dye and its removal from aqueous solution by adsorption: A review. *Advances in Colloid and Interface Science, 209*, 172–184.

Yuna, Z. (2016). Review of the natural, modified, and synthetic zeolites for heavy metals removal from wastewater. *Environmental Engineering Science, 33*, 443–454.

Zaarour, M., Dong, B., Naydenova, I., Retoux, R., & Mintova, S. (2014). Progress in zeolite synthesis promotes advanced applications. *Microporous and Mesoporous Materials, 189*, 11–21.

Zhao, H., Deng, Y., Harsh, J., Flury, M., & Boyle, J. (2004). Alteration of kaolinite to cancrinite and sodalite by simulated Hanford waste and its impact on cesium retention. *Clays Clay Minerals, 52*, 1–13.

(*Received 8 March 2018; revised 3 December 2018; AE: P. Ryan*)